Article:
Zhang, ZQ and Meng, X (2015) Use of an inertial/magnetic sensor module for pedestrian tracking during normal walking. IEEE Transactions on Instrumentation and Measurement, 64 (3). pp. 766-783. ISSN: 0018-9456

https://doi.org/10.1109/TIM.2014.2349211

Use of an Inertial/Magnetic Sensor Module for Pedestrian Tracking during Normal Walking

Zhi-Qiang Zhang* and Xiaoli Meng*

***Abstract*—The ability to track pedestrians without any infrastructure support is required by numerous applications in the healthcare, augmented reality, and entertainment industries. In this paper, we present a simple self-contained pedestrian tracking method using a foot-mounted inertial and magnetic sensor module. Traditional methods normally incorporate double integration of the measured acceleration, but such methods are susceptible to the acceleration noise and integration drift. To avoid this issue, alternative approaches which make use of walking dynamics to aggregate individual stride have been explored. The key for stride aggregating is to accurately and reliably detect stride boundary and estimate the associated heading direction for each stride, but it is still not well solved yet due to sensor noise and external disturbance. In this paper, we propose to make use of the inertial sensor and magnetometer measurements for stride detection and heading direction determination. In our method, a simple and reliable stride detection method, which is resilient to random bouncing motions and sensor noise, is designed based on gyroscope and accelerometer measurements. Heading direction is then determined from the foot's orientation which fuses all the three types of sensor information together. The proposed pedestrian tracking method has been evaluated using experiments, including both short distance walking with different patterns and long distance walking performed indoors and outdoors. The good experimental results have illustrated the effectiveness of the proposed pedestrian tracking method.**

***Index Terms*—Sensor fusion, stance detection, heading, stride counting, pedestrian navigation.**

I. Introduction

The ability to track pedestrians without any infrastructure support is required by numerous applications in the healthcare, augmented reality, and entertainment industries [1] [2]. Until now, current outdoor position tracking technologies mainly rely on satellite navigation systems, such as GPS and GNSS, which normally require an unobstructed line of sight to four or more satellites [3]. However, in urban and indoor environments, satellite signals are unreliable or even unavailable due to the signal attenuation caused by buildings, tunnels, and other construction materials. Although the integration of the satellites and ground base stations can solve this problem, the construction of the base stations is very expensive. Alternative solutions, such as fingerprinting approach and trilateration approach, have been proposed so far. The fingerprinting approach can deliver satisfactory localization accuracy, but it requires complicated setup and high labor input to collect location fingerprints [4] [5]. Similarly, the trilateration method can also achieve relative high localization accuracy, but it requires the coverage of at least three line-of-sight ranging beacon nodes at any point in the service area [6] [7]. Moreover, determination of the locations of the beacon nodes is not easy at all in practice. In summary, although these two approaches can achieve reasonable accuracy, both of them need extra infrastructure support, which impose tremendous challenges for routine use [8].

In recently years, the dead-reckoning approach for pedestrian tracking has attracted extensive research attentions due to its low requirement of infrastructure support. Starting at a known initial user location, a typical dead-reckoning system relies on different sensors to update the location information by adding the current estimated displacement to the previously estimated location [9] [10]. Since the inertial/magnetic measurement unit can work in arbitrary unprepared indoor and outdoor environments, it has been widely applied for self-contained pedestrian tracking. A typical inertial/magnetic measurement unit contains a triaxial accelerometer, a triaxial angular rate sensor, and a triaxial magnetometer, and these sensor units are already commercially available on the market at reasonable cost [11] [12] [13]. The basic idea of the inertial/magnetic measurement unit-based pedestrian tracking is to integrate the measured acceleration twice to estimate distance/position. However, any small acceleration bias error can make the position error increase exponentially; therefore, zero-velocity updates (ZUPTs) are commonly employed to mitigate this problem by resetting the accumulated error [14] [15]. This technique exploits the intrinsic property of pedestrian walking: there are repeated recognizable periods when the foot stays stationary on the ground, during which the velocity and acceleration of the foot are zero. Extensive research has been performed on how to use ZUPTs for accurate position estimation. For example, both Ojeda *et al.* [16] and Bebek *et al.* [17] simply reset the integrated velocity to zero during the zero velocity phases. Foxlin [18] and Godha *et al.* [19] introduced ZUPTs as pseudo-measurements into an extended Kalman filter as the navigation error corrector. Instead of simply resetting the accumulated velocity error periodically, Yun *et al.* [20] further improved the idea of ZUPTs and applied a time variant acceleration bias error to revise the acceleration in the swing phases. Although the removal of the acceleration bias error can significantly improve the accuracy of position tracking, it is still problematic for long distance tracking. Similarly, both Schepers *et al.* [21] and Floor-Westerdijk *et al.* [22] proposed to use high pass filters to remove the bias error. The integrated velocity and the integrated position were high-pass filtered by first-order recursive Butterworth filters

Manuscript received January 22, 2014; revised April 23, 2014 and Jun 8, 2014; accepted August 06, 2014. *Asterisk indicates the joint first authors.*

Z.-Q. Zhang is with the Department of Computing, Imperial College London, SW7 2AZ London, U. K. (e-mail: z.zhang@imperial.ac.uk).

X. L. Meng is with the Institute for Infocomm Research, Singapore.

to alleviate the integration drift, but it is quite challenging to determine the cut-off frequencies of the filters, which makes this method not straightforward to use in practice. However, all the aforementioned acceleration double integration methods assumed that the gravitational acceleration could be removed from the accelerometer signal to obtain the motion acceleration, but such procedure is extremely difficult due to sensor bias and noise.

Alternative approach is to make use of walking dynamics to determine pedestrian location by aggregating individual stride, and the key is to accurately and reliably detect stride boundary and estimate the associated heading direction for each stride [23] [24]. Traditional stride detection typically relies on peak detection/zero-cross over the accelerometer data only, which is sensitive to noise and other irrelevant motion, producing a high rate of false positives, while the heading direction is mainly derived from a magnetometer compass, which is susceptible to metal material disturbance [25]. In this paper, we propose to make use of the inertial sensor and magnetometer measurements for stride detection and heading direction determination. In our method, a simple and reliable stride detection method, which is resilient to random bouncing motions and sensor noise, is designed based on both gyroscope and accelerometer measurements. Heading direction is determined from the foot's orientation which fuses of all the three types of sensor information. The proposed pedestrian tracking method has been evaluated using experiments, including both short distance walking with different patterns and long distance walking performed indoors and outdoors. The good experimental results have illustrated the effectiveness of the proposed pedestrian tracking method.

The rest of the paper is organized as follows: Section II describes the normal walking data acquisition and the stride-counter based pedestrian tracking methods. Experimental results and discussions are described in Section III while conclusion is provided in Section IV.

II. Methods

A. Data Acquisition

The inertial/magnetic sensor module used in the data collection is the sensor chip ADIS16405 from Analog Devices, which contains a triaxial accelerometer, triaxial gyroscope and triaxial magnetometer [26]. The sensor module was connected to a base station by SPI serial data bus, which controlled the data collection and sent the data to PC for offline processing through Bluetooth. During the data collection, the sensor node was placed on the foot as shown in Fig. 1(a).

Two types of walking protocols were designed: short distance walking and long distance walking. Subjects were instructed to walk along the predefined path between the start and end points during walking. For short distance walking, subjects can choose from the following three patterns: 1) walk in a straight line for 15m; 2) walking in a straight line for 10m, and back to the starting point with a turn of 180°; 3) walk in a circle with radius of 3m. For the long distance walking, the subjects can select walking in the corridor for 130m or walking outside for 330m. At least five trials were performed for each walking pattern for statistic analysis.

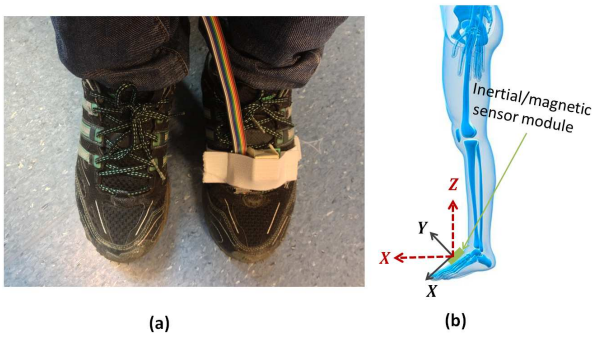

Fig. 1. (a) The attachment of a sensor module on the foot of the subject.(b) The illustration of the coordinate systems. The body coordinate system is given in red dashed lines: X axis pointing the forward direction of the subject, Z axis pointing up and Y axis (not given in the figure) pointing left to form a right hand system, while the sensor coordinate system is given in black solid lines representing the sensor unit sensitivity axes. At the initial position of each trial, the global coordinate system and body coordinate system coincide with each other.

B. Data Analysis

In this section, we will describe how to extract stride length and heading direction information from the inertial/magnetic sensor measurements. Since these parameters are related to each stride, we will introduce how to segment walking steps into strides.

Before we start to introduce the data analysis method, three coordinate systems are defined: 1) the global coordinate system: the reference coordinate system which will remains unchanged during each trial; 2) body coordinate system: coordinate system of the foot segment, X axis pointing the forward direction of the subject, Y axis pointing left and Z axis pointing up. As shown in the Fig. 1(b), the global coordinate system and body coordinate system coincide with each other at the initial position of each trial; 3) sensor coordinate system: three orthogonally axes of the mounted sensors. To facilitate our analysis, all the sensor data needs to be transformed to the body coordinate system before processing, which can be achieved by sensor to body alignment calibration [27].

1) Stride Detection: The gait cycle/stride is used to describe the complex activity of walking. This cycle/stride describes the motions from initial placement of the supporting heel on the ground to when the same heel contacts the ground for a second time. In general, our human gait cycle has two basic components: swing phase and stance phase. During the swing phase, the foot is in the air for lower limb advancement, while during the stance phase, the foot is in contact with the ground.

Previous studies tend to place the sensor node at waist area [23] [24], and only the accelerometer measurements can be used for stride detection since the waist keeps moving all the time during walking. However, when we place the sensor node on the foot, it will have a short stationary period within each stance phase; therefore, we can also use the gyroscope measurements for stride detection to increase the robustness. As shown in Fig. 2, when the foot stays stationary on the ground, the accelerometer only measures the gravity and the gyroscope readings should sense no angular movement;

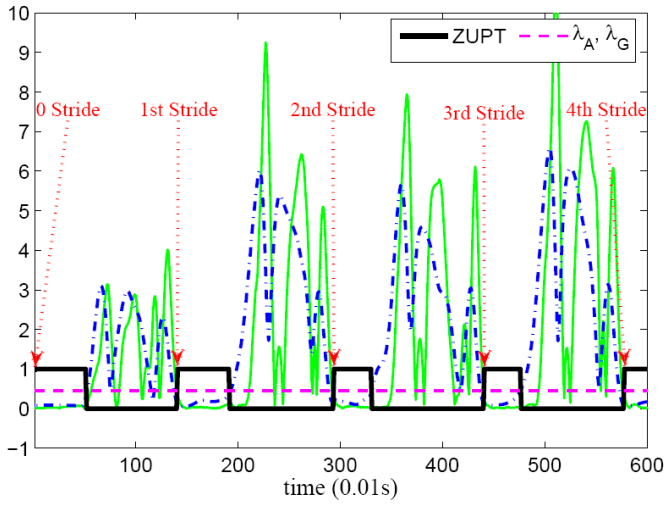

Fig. 2. The detection results of the strides. Green line: $\left|\left\|z_{A,t}\right\| - g\right|$; blue dash-dotted line: $\left|\left\|z_{G,t}\right\|\right|$; red dotted arrows: stride indices. λ_A and λ_G are set to the same value.

therefore, a simple stance phase detector can be designed as:

$$\text{Stance} = \begin{cases} 1, & \left|\left\|z_{A,t}\right\| - g\right| < \lambda_A \text{ and } \left\|z_{G,t}\right\| < \lambda_G \\ 0, & \text{else} \end{cases} \tag{1}$$

where $z_{A,t}$ is the accelerometer measurement at time t, while the $z_{G,t}$ is the gyroscope reading at time t, $\|\cdot\|$ and $|\cdot|$ are the magnitude and absolute operations, respectively, and g denotes the gravity magnitude. λ_A and λ_G are the predefined thresholds which are set to the same value empirically in this paper. As shown in the figure, the first point of each stance phase is taken as the end of a stride or as the start of a new stride.

2) Stride length estimation: Stride length may vary from stride to stride even for the same pedestrian, but it has shown that the walking speed strongly influences the amplitude of the acceleration signal. Therefore, the stride length S_k can be approximated with minimum latency by using a simple formula [28] [23]:

$$S_k = \Gamma \cdot \sqrt[4]{z_{A,k}^{\max} - z_{A,k}^{\min}} \tag{2}$$

where $z_{A,k}^{\max}$ (or $z_{A,k}^{\min}$) is the maximum (or minimum) vertical acceleration in the stride k, and Γ is a constant. Although the parameter Γ is user specific, our test results show that it does not vary too much from person to person. In our experiment, the value of the subject-dependent parameter Γ can be determined by obtaining the actual distance d covered by a calibration walking trial of N strides.

3) Heading direction determination: Since the heading direction is critical to the location estimation performance, it should be determined as accurate as possible using all the sensor measurements together. Here, the heading direction is determined from the foot's orientation which fuses all the sensor information. Given the gyroscope measurement $z_{G,t}$, the foot's orientation q_t at time step t can be predicted as [29]:

$$q_t = \exp\left(\frac{1}{2}\Omega\left[z_{G,t}\right]\delta_t\right) q_{t-1} + w_t \tag{3}$$

where $q_t = [q_{1,t}, q_{2,t}, q_{3,t}, q_{4,t}]^T = \left[e_t^T, q_{4,t}\right]^T$, $q_{4,t}$ and $e_t = [q_{1,t},\ q_{2,t},\ q_{3,t}]^T$ are the scalar part and vector part of q_t, respectively. δ_t is the sampling interval (set to 0.01s in our implementation), and $\Omega\left[z_{G,t}\right]$ is a 4×4 skew symmetric matrix as in

$$\Omega\left[z_{G,t}\right] = \begin{bmatrix} -\left[z_{G,t}\times\right] & z_{G,t} \\ -z_{G,t}^T & 0 \end{bmatrix}, \tag{4}$$

$[\times]$ represents the cross product operator [30], and w_t is a zero-mean Gaussian noise with covariance matrix $\mathbf{Q}$.

The gravity acceleration and earth magnetic field strength are used to compensate for the predicted quaternion to get drift-free orientation estimation. Given a quaternion q_t and the reference magnetic vector r_M, the measurement equation of the magnetometer signal $z_{M,t}$ can be defined as:

$$z_{M,t} = C(q_t)\, r_M + n_{M,t} \tag{5}$$

where $C(q_t)$ is the corresponding rotational matrix of the quaternion q_t [30]:

$$C(q_t) = \left(q_{4,t}^2 - e_t^T e_t\right)\mathbf{I}_3 + 2e_t e_t^T - 2q_{4,t}\left[e_t\times\right] \tag{6}$$

where $n_{M,t}$ is the magnetometer measurement noise with zero mean and covariance matrix $\mathbf{\Sigma}_{M,t}$. Similarly, the measurement equation of the accelerometer signal $z_{A,t}$ can be defined as:

$$z_{A,t} = C(q_t)\, g_0 + n_{A,t} \tag{7}$$

where $n_{A,t}$ is the accelerometer measurement noise with covariance $\mathbf{\Sigma}_A$; and g_0 denotes the reference gravity vector.

From (5) and (7), the sensor measurement model is given by:

$$\begin{aligned} z_t &= \begin{bmatrix} z_{M,t} \\ z_{A,t} \end{bmatrix} = f(x_t) + n_t \\ &= C(q_t) \cdot \begin{bmatrix} r_M \\ g_0 \end{bmatrix} + \begin{bmatrix} n_{M,t} \\ n_{A,t} \end{bmatrix} \end{aligned} \tag{8}$$

The covariance matrix of the sensor measurement noises n_t, denoted by $\mathbf{R}_t$, is given by:

$$\mathbf{R}_t = \begin{bmatrix} \mathbf{\Sigma}_{M,t} & \mathbf{0}_{3\times3} \\ \mathbf{0}_{3\times3} & \mathbf{\Sigma}_A \end{bmatrix} \tag{9}$$

Once the prediction model and sensor measurement model are defined, an Unscented Kalman filter (UKF) can be used to fuse all the sensor measurements together for orientation estimation. In practice, body motion acceleration and magnetic disturbances can affect the performance of the UKF. To make the UKF resilient to body motion acceleration and magnetic disturbance, we applied the adaptive weighting mechanism to adjust the corresponding measurement covariance matrix presented in our previous work [31] [32]. After the measurement covariance adjustment, a standard UKF can be employed to deal with the filtering [33].

When a stride is detected, the heading angle θ_k can be extracted from the orientation of the k^{th} stride, represented by q_{S_k}, as given in:

$$\theta_k = \text{atan2}\left(2(q_{S_k,4}q_{S_k,3} + q_{S_k,1}q_{S_k,2}), 1 - 2(q_{S_k,2}^2 + q_{S_k,3}^2)\right) - \theta_0 \tag{10}$$

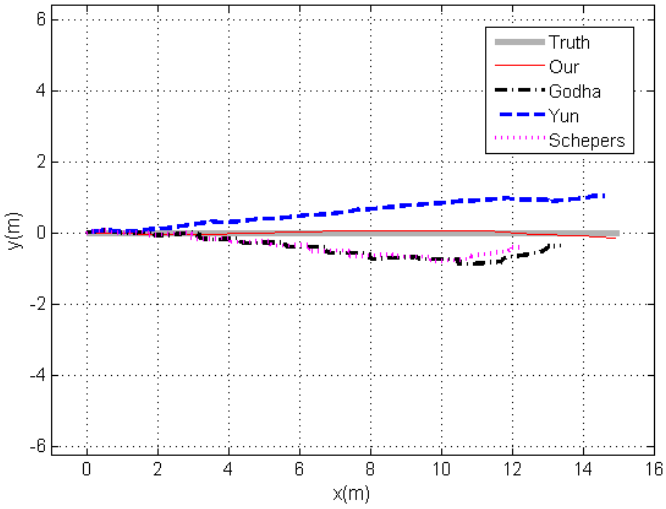

Fig. 3. One example of the estimated displacement results for walking in a straight line for 15m.

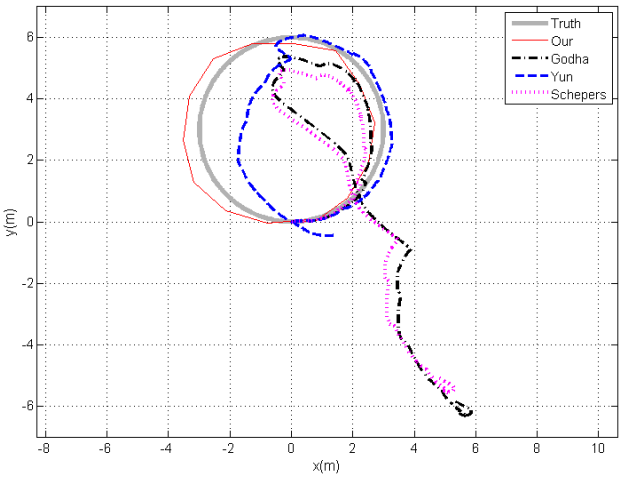

Fig. 5. One example of the estimated displacement results for walking in a circle with radius of 3m.

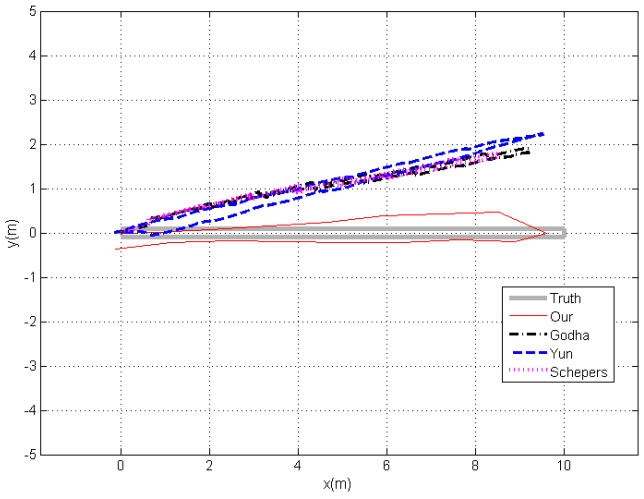

Fig. 4. One example of the estimated displacement results for walking in a straight line for 10m, and back to the starting point with a turn of 180°.

where θ_0 is the initial heading angle. Thus, the pedestrian location $l_{p,k}$ can be updated by:

$$l_{p,k} = l_{p,k-1} + [S_k \cos\theta_k, S_k \sin\theta_k] \tag{11}$$

where $l_{p,k-1}$ is the location estimation of the previous stride.

III. Experimental Results and Discussion

A. Experimental Demonstration

In order to better illustrate the performance of the pedestrian tracking, a comparison study between the state-of-the-art ZUPT-based methods and our method was carried out. In our experiments, three ZUPT-based methods were implemented: Godha's method [19] which simply resets the velocity drift to zero during the stance phases; Yun's method [20] which applies a time-variant acceleration bias error to remove velocity drift; and Schepers' method [21] [22] which uses high pass filters to remove velocity drift. In what follows, 'Truth' represents the marked trajectory that the subjects need to follow; 'Our' shows the tracking results of our method, while 'Godha', 'Yun' and 'Schepers' stand for the corresponding ZUPT-based methods, respectively.

1) Short distance walking: For short distance walking, three walking patterns were designed for the subjects to follow as described in Section II.A. Figs. 3–5 give the exemplary results of the pedestrian location estimation using different methods. In these figures, the thick grey solid lines represent the predefined path that the subjects need to follow, while the thin solid lines indicate the estimated trajectory using our proposed method. The dotted-dashed lines, dashed lines and dotted lines illustrate the position estimation results of the three ZUPT-based methods: Godha's method, Yun's method and Schepers' method, respectively. The statistic results of the position errors for these three walking patterns are given in Table I. For the straight line walking, the path is not a closed-loop trajectory, and the position error is calculated using the difference between the estimated final position and the truth final position. For the other walking patterns with closed-loop trajectories, the position error is evaluated by the difference between the starting and final positions. Table I also shows the average position errors and the standard derivations over the 5 trials. The average position error of the proposed method for straight line walking is 0.51±0.18m, for walking with 180° turn is 0.68±0.45m, and for walking in a circle path is 0.70±0.41m, respectively. As we can see from the figures and the table, it is evident that the proposed stride-counter based method outperforms all the ZUPT-based methods.

2) Long distance walking: In order to further validate the feasibility of our method for long-term walking tracking, both indoor and outdoor long distance walking were conducted. The indoor experiment was carried out in the corridors in our laboratory, while the outdoor experiment was conducted outside our department building. The predefined walking paths are shown by the thick solid lines in Fig. 6 and Fig. 7. From the start position (0,0) in the plot, the subjects walk along the path, make several turns and then walk back to the starting position. To facilitate the waling process, distinctive points along the

TABLE I
ABSOLUTE INITIAL-FINAL POSITION ERROR FOR SHORT DISTANCE WALKING (UNIT: M)

Position error	line				turn				circle			
	Our	Godha	Yun	Schepers	Our	Godha	Yun	Schepers	Our	Godha	Yun	Schepers
Trial 1	0.24	2.19	2.20	3.08	0.21	1.20	0.48	1.03	1.37	3.97	0.59	3.72
Trial 2	0.70	1.85	3.80	2.92	0.91	0.65	1.01	0.38	0.27	6.53	2.81	6.62
Trial 3	0.19	1.70	1.11	2.78	0.99	0.54	0.39	0.33	0.26	6.15	0.90	5.80
Trial 4	0.54	1.63	2.90	2.76	0.64	0.31	0.58	0.58	7.82	1.52	6.88	
Trial 5	0.42	1.23	1.82	2.3	0.37	0.89	0.13	0.79	0.95	5.44	4.43	3.73
mean±std	0.42±0.21	1.72±0.35	2.36±1.03	2.77±0.29	0.58±0.35	0.79±0.27	0.47±0.33	0.62±0.29	0.69±0.48	5.98±1.42	2.05±1.58	5.35±1.54

TABLE II
ABSOLUTE INITIAL-FINAL POSITION ERROR FOR LONG DISTANCE WALKING (UNIT: M)

Position error	indoor				outdoor			
	Our	Godha	Yun	Schepers	Our	Godha	Yun	Schepers
Trial 1	3.54	14.68	4.45	13.54	5.92	16.18	11.21	15.09
Trial 2	4.89	7.18	4.15	6.72	11.13	13.75	14.75	13.31
Trial 3	5.76	6.69	5.89	6.25	6.48	12.09	14.37	11.29
Trial 4	4.61	13.56	7.52	12.48	5.79	14.53	12.48	12.32
Trial 5	4.06	18.71	4.80	17.55	6.31	11.70	8.33	11.38
mean±std	4.57±0.84	12.16±5.15	5.36±1.37	11.31±4.79	7.13±2.26	13.65±1.83	12.23±2.61	12.68±1.58

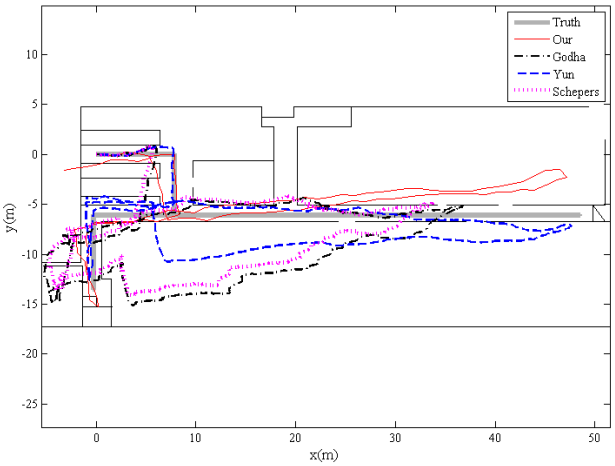

Fig. 6. One example of the displacement estimation for the indoor experiments.

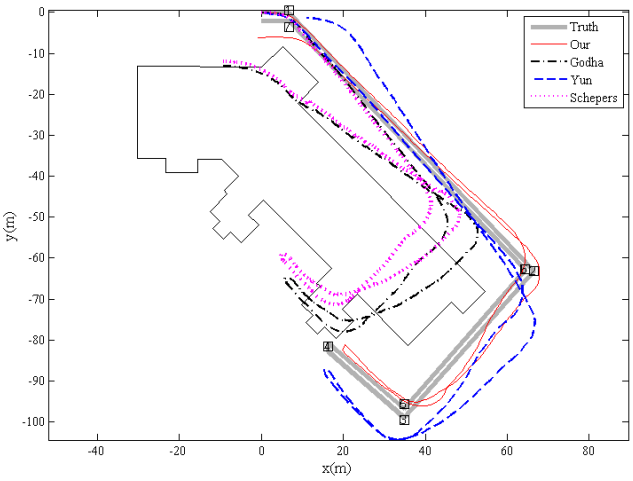

Fig. 7. One example of the displacement estimation for the outdoor experiments. The actual positions of the 7 important points are marked by the square number plates.

walking path are marked on the floor to guide the subjects to walk along the path. Similar to the short distance walking, the thick grey solid lines in Fig. 6 and Fig. 7 represent the predefined path that the subjects need to follow, and the thin solid lines indicate the estimated trajectory using our proposed method. The dotted-dashed lines, dashed lines and dotted lines illustrate the position estimation results of the three ZUPT-based methods: Godha's method, Yun's method and Schepers' method, respectively. Both indoor and outdoor walking experiments are repeated 5 times, and the statistic position errors are shown in Table II. For our proposed method, the averaged error for 3 minutes indoor walking is 4.57±0.84m, and for 6 minutes outdoor walking is 7.13±2.26m. The comparison results of the average position errors among the four methods indicate our method has achieved the highest accuracy in the long-term experiments.

B. Discussion

In our previous analysis, we only use the position differences between the starting and final points to evaluate the performance of the proposed pedestrian tracking algorithm. Although it is commonly recognized in the accuracy assessment of the pedestrian tracking [17] [20] [34], the tracking performance may not be fully exploited by this method since it ignores the possible deviation of the other points from the walking path. Therefore, more points should be extracted from the walking path for the performance evaluation. One possible way is to choose the critical turning points from the path of the ground truth. Taking the outdoor long-term walking as an example, except the starting and final points, 7 more points can be used for evaluation, which are marked by the square number

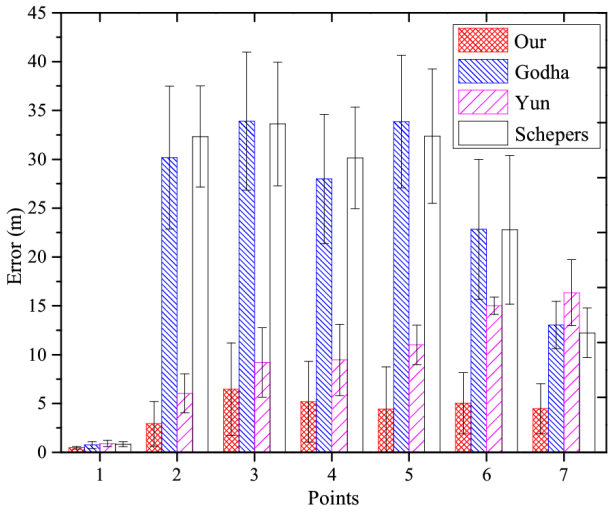

Fig. 8. The distance errors between the estimated positions and actual positions of the 7 important points.

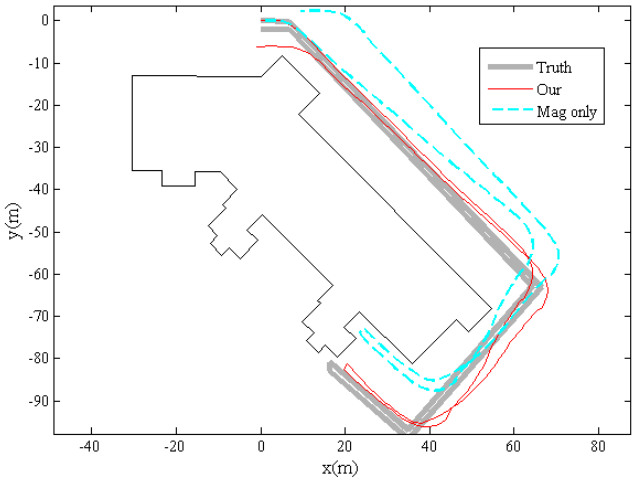

Fig. 9. The illustration of the displacement estimation results using the magnetometer only for heading direction determination.

plates in Fig. 7. The average distance errors and standard deviations between the estimated positions and actual positions from the 5 trials are shown in Fig. 8. It is evident that although the proposed stride-counter based pedestrian tracking method is very simple for implementation, it still can achieve the best tracking accuracy over the state-of-the-art ZUPT-based methods. Based on the results shown in Tables I–II and Figs. 3–8, it is evident that the Yun's method outperforms the other two ZUPT-based methods. This is mainly because Godha's method only simply reset the velocity to zero during the stance phases and the accumulated drift during the swing phases is included in the location estimation. Although Schepers' method applied first-order recursive Butterworth high pass filters to remove the drift caused by the acceleration bias in the integrated velocity, the filters can't remove the integration drift during the stance phases due to the difficulty choosing the cut-off frequency. Yun's method applied an acceleration bias variable not only to revise the integrated velocity during the swing phases, but also to set the velocity to zero during the stance phases, which can significantly improve the accuracy of position tracking over the other two ZUPT-based methods. However, all the ZUPT-based methods assume that the gravitational acceleration can be removed from the accelerometer signal to obtain the motion acceleration, but such procedure is extremely difficult, and the errors in the motion acceleration can't be fully compensated by the zero velocity constraint. Instead of integrating the measured acceleration, our proposed method make use of the walking dynamics contained in the sensor signals, such as frequency, maximum/minimum amplitude, which can avoid motion acceleration derivation and integration drift. Therefore, good pedestrian tracking accuracy can be achieved.

The stride-counter based methods also have some pitfalls over the ZUPT-based methods. The major disadvantage of the stride-based method is it can only work on the level ground or the 2D environment. In our experiments, only X axis and Y axis displacements were estimated, while the Z axis movement was ignored. However, the ZUPT-based methods can not only estimate the movement in X and Y axes, but also can estimate the displacements in Z axis. Foxlin [18] and Yun et al. [20] have demonstrated it is possible that the ZUPT-based methods can be applied for the downstairs/upstairs walking tracking, which is beyond the ability of stride-based methods. The second disadvantage of the stride-based method is that it can only work for normal forward walking scenarios, since it is not applicable to the other walking patterns, like backwards walking and sideways walking. In theory, the ZUPT-based methods should also be able to provide reasonable displacement estimation for the backwards walking and sideways walking, although we haven't found any study evaluating such walking patterns. The third disadvantage of the stride-based method is its low updating frequency. From the Fig. 4 and Fig. 5, it is very clear that the stride-based method can only provide one location estimation per stride while the ZUPT-based method can give 100 location updates per second. Therefore, to overcome the pitfalls of the stride-based method and also to make use of the stride-based method, our future work will be to integrate the ZUPT-based method and the stride-based method together, and it can be expected that the tracking accuracy could be further improved.

To further illustrate the effectiveness of the proposed stride-based method, we have also evaluated the characteristics of the two key steps involved in our method: the stride detection, and heading direction determination. In the stride detection step, we used the accelerometer and gyroscope measurements together for the stance phase detection, and no miss-detection or false positive detection has been found in our experiments. However, we also used the accelerometer alone for stride detection, and approximately 10% of the detected strides are false positive due to noise and other irrelevant motion, which means that the incorporation of gyroscope measurements can improve the robustness of the stride detection. We also applied the magnetometer only for the heading direction determination. Fig. 9 shows an example of the outdoor walking results. It is obvious that the tracking performance using the magnetometer

only for heading direction determination is much worse than that of using all the sensor measurements. The reason is that when there is magnetic disturbance, the gyroscope and accelerometer can compensate for such disturbances and still provide accurate heading directions.

IV. Conclusion and Future Work

This paper provided an alternative approach for pedestrian tracking by investigating the usage of the stride length and heading direction to avoid the motion acceleration derivation and excessive double acceleration integration drift. In our method, a simple and reliable stride detection method, which is resilient to random bouncing motions and sensor noise, was designed based on both gyroscope and accelerometer measurements. Heading direction was then determined from the foot's orientation which fuses of all the three types of sensor information. The proposed pedestrian tracking method has been evaluated using experiments, including both short distance walking with different patterns and long distance walking performed indoors and outdoors. The good experimental results have illustrated the effectiveness of the proposed pedestrian tracking method.

Our future work will focus on extending our current method by incorporating the ZUPT-based method in. More walking patterns experiments, like backwards walking, sideways walking and stair climbing, and longer distance waling trials will be carried out to further evaluate our method. The usage of map information for pedestrian navigation will also be explored in the future.

References

[1] Y. Jin, W.-S. Soh, M. Motani, and W.-C. Wong, "A robust indoor pedestrian tracking system with sparse infrastructure support," *Mobile Computing, IEEE Transactions on*, vol. 12, no. 7, pp. 1392–1403, 2013.

[2] Z. Zhang, A. Panousopoulou, and G.-Z. Yang, "Wearable sensor integration and bio-motion capture: A practical perspective," in *Body Sensor Networks*. Springer, 2014, pp. 495–526.

[3] R. Ivanov, "Real-time GPS track simplification algorithm for outdoor navigation of visually impaired," *Journal of Network and Computer Applications*, vol. 35, no. 5, pp. 1559–1567, 2012.

[4] P. Bahl and V. N. Padmanabhan, "Radar: An in-building rf-based user location and tracking system," in *Nineteenth Annual Joint Conference of the IEEE Computer and Communications Societies*, vol. 2, 2000, pp. 775–784.

[5] Widyawana, G. Pirkl, D. Munaretto, C. Fischer, C. An, P. Lukowicz, M. Klepal, A. Timm-Giel, J. Widmer, D. Pesch, and H. Gellersen, "Virtual lifeline: multimodal sensor data fusion for robust navigation in unknown environments," *Pervasive and Mobile Computing*, vol. 8, no. 3, pp. 388–401, 2012.

[6] M. Mirbach and W. Menzel, "A simple surface estimation algorithm for uwb pulse radars based on trilateration," in *Ultra-Wideband (ICUWB), 2011 IEEE International Conference on*. IEEE, 2011, pp. 273–277.

[7] J. Corrales, F. Candelas, and F. Torres, "Hybrid tracking of human operators using IMU/UWB data fusion by a Kalman filter," in *Proc. 3rd ACM/IEEE int. conf. HRI*, Amsterdam, The Netherlands, Mar. 2008, pp. 193–200.

[8] N. Fallah, I. Apostolopoulos, K. Bekris, and E. Folmer, "Indoor human navigation systems: A survey," *Interacting with Computers*, vol. 25, no. 1, pp. 21–33, 2013.

[9] R. Harle, "A survey of indoor inertial positioning systems for pedestrians," *Communications Surveys Tutorials, IEEE*, vol. 15, no. 3, pp. 1281–1293, 2013.

[10] X. Meng, Z.-Q. Zhang, J.-K. Wu, W.-C. Wong, and H. Yu, "Self-contained pedestrian tracking during normal walking using an inertial/magnetic sensor module," *Biomedical Engineering, IEEE Transactions on*, vol. 61, no. 3, pp. 892–899, March 2014.

[11] ProMove-3D. [Online]. Available: http://inertia-technology.com/

[12] Microstrain 3DM. [Online]. Available: http://www.microstrain.com

[13] Z.-Q. Zhang and G.-Z. Yang, "Calibration of miniature inertial and magnetic sensor units for robust attitude estimation," *Instrumentation and Measurement, IEEE Transactions on*, vol. 63, no. 3, pp. 711–718, March 2014.

[14] P. Groves, *Principles of GNSS, Inertial and Multisensor Integrated Navigation Systems*. Boston, London: Artech House, Inc, 2008.

[15] I. Skog, P. Handel, J. Nilsson, and J. Rantakokko, "Zero-velocity detection - an algorithm evaluation," *IEEE Trans. Biomed. Eng.*, vol. 57, no. 11, pp. 2657–2666, 2010.

[16] L. Ojeda and J. Borenstein, "Non-GPS navigation for security personnel and first responders," *J. Navigation*, vol. 60, no. 3, pp. 391–407, 2007.

[17] O. Bebek, M. Suster, S. Rajgopal, M. Fu, X. Huang, M. Cavusoglu, D. Young, M. Mehregany, A. van den Bogert, and C. Mastrangelo, "Personal navigation via high-resolution gait-corrected inertial measurement units," *IEEE T. Instrum. Meas.*, vol. 59, no. 11, pp. 3018–3027, 2010.

[18] E. Foxlin, "Pedestrian tracking with shoe-mounted inertial sensors," *IEEE Comput. Graph.*, vol. 25, no. 6, pp. 38–46, 2005.

[19] S. Godha and G. Lachapelle, "Foot mounted inertial system for pedestrian navigation," *Meas. Sci. Technol.*, vol. 19, no. 7, pp. 075 202:1–9, 2008.

[20] X. Yun, J. Calusdian, E. Bachmann, and R. McGhee, "Estimation of human foot motion during normal walking using inertial and magnetic sensor measurements," *IEEE T. Instrum. Meas.*, vol. 61, no. 7, pp. 2059–2072, 2012.

[21] H. M. Schepers, E. van Asseldonk, J. H. Buurke, and P. H. Veltink, "Ambulatory estimation of center of mass displacement during walking," *Biomedical Engineering, IEEE Transactions on*, vol. 56, no. 4, pp. 1189–1195, 2009.

[22] M. J. Floor-Westerdijk, H. Schepers, P. H. Veltink, E. H. van Asseldonk, and J. H. Buurke, "Use of inertial sensors for ambulatory assessment of center-of-mass displacements during walking," *Biomedical Engineering, IEEE Transactions on*, vol. 59, no. 7, pp. 2080–2084, 2012.

[23] L. Fang, P. J. Antsaklis, L. A. Montestruque, M. B. McMickell, M. Lemmon, Y. Sun, H. Fang, I. Koutroulis, M. Haenggi, M. Xie *et al.*, "Design of a wireless assisted pedestrian dead reckoning system-the navmote experience," *Instrumentation and Measurement, IEEE Transactions on*, vol. 54, no. 6, pp. 2342–2358, 2005.

[24] A. Brajdic and R. Harle, "Walk detection and step counting on unconstrained smartphones," in *Proceedings of the 2013 ACM international joint conference on Pervasive and ubiquitous computing*. ACM, 2013, pp. 225–234.

[25] F. Li, C. Zhao, G. Ding, J. Gong, C. Liu, and F. Zhao, "A reliable and accurate indoor localization method using phone inertial sensors," in *Proceedings of the 2012 ACM Conference on Ubiquitous Computing*. ACM, 2012, pp. 421–430.

[26] Analog Devices ADIS16405. [Online]. Available: http://www.analog.com/

[27] X. Meng, Z. Zhang, S. Sun, J. Wu, and W.Wong, "Biomechanical model-based displacement estimation in micro-sensor motion capture," *Meas. Sci. Technol.*, vol. 23, no. 5, pp. 055 101:1–11, 2012.

[28] J. W. Kim, H. J. Jang, D.-H. Hwang, and C. Park, "A step, stride and heading determination for the pedestrian navigation system," *Journal of Global Positioning Systems*, vol. 3, no. 1-2, pp. 273–279, 2004.

[29] Z.-Q. Zhang and J.-K. Wu, "A novel hierarchical information fusion method for three-dimensional upper limb motion estimation," *Instrumentation and Measurement, IEEE Transactions on*, vol. 60, no. 11, pp. 3709–3719, 2011.

[30] D. Choukroun, I. Bar-Itzhack, and Y. Oshman, "Novel quaternion Kalman filter," *IEEE Trans. Aero. Elec. Sys.*, vol. 42, no. 1, pp. 174–190, 2006.

[31] Z.-Q. Zhang, L.-Y. Ji, Z.-P. Huang, and J.-K. Wu, "Adaptive information fusion for human upper limb movement estimation," *Systems, Man and Cybernetics, Part A: Systems and Humans, IEEE Transactions on*, vol. 42, no. 5, pp. 1100–1108, 2012.

[32] Z.-Q. Zhang, X.-L. Meng, and J.-K. Wu, "Quaternion-based kalman filter with vector selection for accurate orientation tracking," *Instrumentation and Measurement, IEEE Transactions on*, vol. 61, no. 10, pp. 2817–2824, 2012.

[33] E. Wan and R. V. D. Merwe, "The Unscented Kalman filter for nonlinear estimation," in *Proc. IEEE AS-SPCC*, Lake Louise, Alta., Canada, Oct. 2000, pp. 153–158.

[34] A. Ruiz, F. Granja, J. Honorato, and J. Rosas, "Accurate pedestrian indoor navigation by tightly coupling foot-mounted IMU and RFID measurements," *IEEE Trans. Instrum. Meas.*, vol. 61, no. 1, pp. 178–189, 2012.

Zhi-Qiang Zhang received the B.E. degree in computer science and technology from School of Electrical Information and Engineering, Tianjian University, China, in 2005, and the Ph.D. degree from the Sensor Network and Application Research Center, Graduate University, Chinese Academy of Sciences, Beijing, China, in 2010.
He is currently a Research Associate with the Hamlyn Centre for Robotic Surgery, Imperial College, London. His research interests include Body Sensor Network, Information Fusion, Machine Learning and Targets Tracking.

Xiaoli Meng received the B.E. degree in communication engineering from Tianjin University, China, in 2007, and the Ph.D. degree from the Sensor Network and Application Research Center, Graduate University, Chinese Academy of Sciences, Beijing, China, in 2012. After working as a Research fellow in the Department of bioengineering, Nation University of Singapore from 2012 to 2013, she is now a research scientist with the Institute for Infocomm Research, Singapore. Her research interests include human motion tracking, gait analysis, and rehabilitation robotics.